

Coherent Inverse Compton Scattering Responsible for Pulsar Polarized and Unpolarized Emission

To cite this article: Liu Ji-feng *et al* 1999 *Chinese Phys. Lett.* **16** 541

View the [article online](#) for updates and enhancements.

Related content

- [ICS Model of Pulsar Emission](#)
R. X. Xu, J. F. Liu, J. L. Han *et al.*
- [CIRCULAR POLARIZATION IN PULSARS](#)
R. T. Gangadhara
- [Coherence and Pulsar Radio Emission](#)
Bing Zhang, B. H. Hong and G. J. Qiao

Recent citations

- [Scaling Law of Nonlinear Compton Scattering](#)
Wang Ping-Xiao *et al*

Coherent Inverse Compton Scattering Responsible for Pulsar Polarized and Unpolarized Emission *

LIU Ji-feng(刘继锋)¹, QIAO Guo-jun(乔国俊)^{1,2}, XU Ren-xin(徐仁新)¹

¹CAS-PKU Joint Beijing Astrophysics Center & Department of Geophysics, Peking University, Beijing 100871

²CCAST (World Laboratory), P.O.Box 8730, Beijing 100080

(Received 8 January 1999)

A coherent inverse Compton scattering (ICS) mechanism is used to get polarization properties of radio emission of pulsars. It is found that particles moving along a ring with radius $\theta' = 1/(\sqrt{3}\gamma)$ simultaneously contribute via coherent ICS. The circular polarization can be easily gotten as well as linear polarization at the same time. Our theory releases the upper limit of Lorentz factor $\gamma \leq 20$ put by curvature radiation, and γ may take several thousands in ICS. Furthermore, subpulse position angles do take diverse values, while mean position angle is associated with the projection of magnetic field lines. So it is natural to get commonly-seen S-shaped swing of mean position angles. Finally we present a simulation for position angle rotation, linear polarization, circular polarization of PSR1508+55, which means that the coherent ICS may be responsible for radio emission.

PACS: 97.60.Gb, 42.68.Mj, 34.50.Dy

Polarization properties of radio pulsars play a key role in understanding the magnetospheric structure and radio emission mechanisms. Early studies usually quoted coherent curvature radiation, if not only as the main emission mechanism for relativistic particles in the superstrong magnetic field of pulsar. Recent researches have argued against its role in the emission processes. Lesch *et al.*¹ pointed out that coherent curvature radiation cannot supply sufficient radio luminosity. Zhang and Qiao² show that inverse Compton scattering (ICS) plays a more important role than curvature radiation in inner gap sparking processes. Rankin³ pointed out that pulsar's emission beams may consist of a solid core and two hollow cones phenomenologically, which rules out the hollow cone model predicted by curvature radiation.⁴ Qiao^{5,6} initially pointed out that ICS may be responsible for the pulsar radio emission. Qiao and Lin⁷ presented a model based on ICS, which gives sufficient radio luminosity and one core plus two cones emission beam. They also pointed out that a slight degree of coherence is also needed. Xu⁸ studies the coherent ICS process using classical electrodynamics, found that coherent superposition of scattered electromagnetic waves could lead to circularly polarized components. He also simulated a situation in which six bunches of outmoving electrons (or positrons) near the pulsar surface contribute simultaneously to what we observe and got different types of subpulses.

In this paper, the assumption in Xu⁸ on the emission height, the Lorentz factor and bunch numbers are released. The Lorentz factor is taken to be 1000, a more reasonable value.² The emission heights are determined in the framework of ICS model, which are about 10 km for core emission, several tens kilometers for inner cone and several hundreds for out cone. It

is found that it is natural to observe circular polarization as well as linear polarization, and results for subpulses and mean profiles are quite consistent with observations.

Inner gap was argued to exist by many authors.^{7,9} The continuous formation and breakdown ("sparkings") of the inner gap provide both low frequency waves with $\omega_0 \sim 10^6 \text{ rad}\cdot\text{s}^{-1}$ and outstreaming relativistic particles with $\gamma \sim 10^3$. According to ICS mode,⁵⁻⁷ the low frequency waves will be scattered by relativistic particles to observed radio waves i.e., ICS. Such a process can be considered in a classical electrodynamic way. First we transfer the low frequency waves into the rest frame of the relativistic particles in which the particles radiate just like a dipole along the magnetic field line, then we transfer the dipolar radiation field from the rest frame to the lab frame. The frequency ω' and the electric field amplitude \mathbf{E} of the scattered waves read⁸

$$\omega' = \frac{2}{1 + \gamma^2 \theta'^2} \omega_0 \gamma^2 (1 - \beta \cos \theta_i), \quad (1)$$

$$\mathbf{E} = C \frac{\sin \theta'}{\gamma^2 (1 - \beta \cos \theta')^2} e^{i(\frac{\omega_0}{c} R - \frac{\omega'}{c} \mathbf{R} \cdot \mathbf{n} + \phi_0)} \mathbf{e}_s, \quad (2)$$

where \mathbf{n} is the observing direction, \mathbf{R} the low frequency wave vector, θ_i the incoming angle between \mathbf{R} and particle's moving direction \mathbf{n}_e , $\cos \theta_i = \mathbf{R} \cdot \mathbf{n}_e$, θ' the angle between \mathbf{n}_e and \mathbf{n} , $\cos \theta' = \mathbf{n} \cdot \mathbf{n}_e$, γ the Lorentz factor of the particle which takes $\sim 10^3$.

Note that the amplitude of the scattered wave reaches its sharp-pointed maximum when $\theta' = 1/(\sqrt{3}\gamma)$, and it is reasonable to simplify that the scattered waves are mainly in a hollow cone along \mathbf{n}_e with half angle $\theta' = 1/(\sqrt{3}\gamma)$. As a result, the scattered

* Supported in part by the National Natural Science Foundation of China under Grant No.19673001, the Climbing Project—National Key Project for Fundamental Research of China, and the Doctoral Program Foundation of Institution of Higher Education in China.

frequency ω' is

$$\omega' = \frac{3}{2} \omega_0 \gamma^2 (1 - \beta \cos \theta_i), \quad (3)$$

where both γ and $\cos \theta_i$ are functions of emission height r , $\cos \theta_i$ is determined by the geometry of magnetic field, which takes⁷

$$\cos \theta_i = \frac{2 \cos \theta + (R_0/r)(1 - 3 \cos^2 \theta)}{\sqrt{(1 + 3 \cos^2 \theta)[1 - 2(R_0/r) \cos \theta + (R_0/r)^2]}}. \quad (4)$$

While moving out and losing energy via ICS, the particle undergoes a decay in γ . A simple assumption⁷ is introduced as

$$\gamma = \gamma_0 \left[1 - \xi \frac{r - R_0}{R_e} \right], \quad (5)$$

where γ_0 is Lorentz factor of the particles and ξ present the energy loss. Since ω' is a function of emission height, we can determine where the bunch of particles can be seen at observing frequency ω' . As pointed out,⁷ there are generally three possible emission zones, corresponding to core, inner and outer cones in Rankin's term.³ We emphasize that if a bunch of particles can be seen, the scattered waves can be received from a ring of particles with the angle $\theta' = 1/(\sqrt{3}\gamma)$ between the moving directions and the observing direction. The scattered electromagnetic waves can be superposed coherently if they are emitted from the processes in which low frequency waves from one sparking point are scattered by a ring of particles. If low frequency waves are from different sparking points, the scattered waves cannot be treated coherently because their initial phase ϕ_0 in Eq. (2) are randomly different. The coherent superposition of scattered waves will result in circular polarization as well as linear polarization. We present in the following numerical simulations to outline the polarization properties of radio emission via ICS process.

Consider a stable sequence of bunches of particles moving along given field lines, they will emit via ICS process at fixed heights determined by Eq. (3) and form three "microbeams" (core and two cones) spanning a few of degrees. Coherent superposition of radiation from all the particles with observing frequency ω' results in a microbeam pattern with both linear and circular polarization. Our numerical simulation shows that the core microbeam is generally significantly circularly polarized; the inner cone microbeam is less circularly polarized, the outer cone microbeam is hardly circularly polarized; which is in agreement with the analyses of Rankin^{3,10} and most recent works.¹¹⁻¹³ We take that the line of sight sweeping across such a microbeam results in a subpulse. If the line of sight sweeps across the center of a core or inner cone microbeam, the circular polarization of the subpulse will experience a central sense reversal, or else it will retain within the subpulse its sense, either left hand or

right hand according to its traversal relative to the microbeam. Figure 1 shows a variety of possible circular polarization patterns of subpulses.

The width of subpulse is generally 2–3 deg and led early authors to requirement that γ be less than several tens, because they thought the width is associated with $1/\gamma$. In our deduction a subpulse is produced by a bunch of particles along certain field lines. The width of subpulse is mainly determined by the dimension of the bunch, the radius of which near the star surface is taken 10 m as the height of inner gap. Such a radius corresponds to a width of more than one degree (as shown in Fig. 1) for subpulse from core emission and slightly larger for subpulse from cones. Since the association between the width of subpulse and γ is discarded, the upper limit upon γ can be released to 10^3 , which is the quantity we take in this paper.

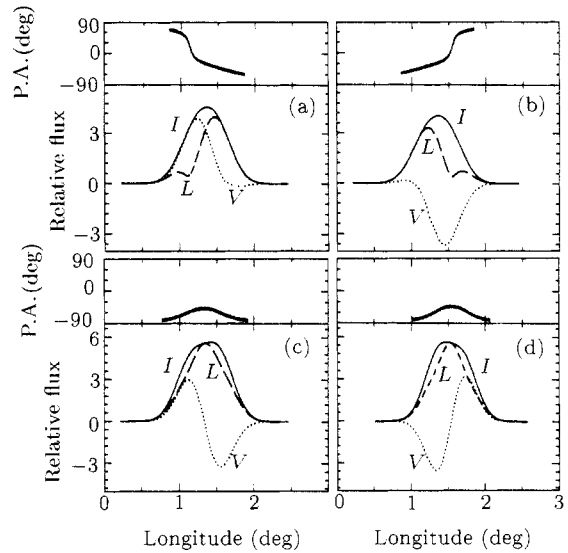


Fig. 1. Possible patterns of subpulse polarization. I , L , and V are the Stokes parameters. The sense of circular polarization retains left hand (LH) in (a) and right hand (RH) in (b). The sense reverses from LH to RH in (c) and from RH to LH in (d). The variation of position angle (P. A.) for (c and d) is as small as a few tens of degrees, but rather larger for (a and b). The differences are due to traversal effects. In the simulation the pulsar period is typically taken to be one second, $\gamma_0 = 1000$, $\xi = 0.002$, the observing frequency is 1 GHz.

Subpulse position angles show diverse values, which are generally centered at the projection of the magnetic field. The variation range of position angles is quite small for subpulses from outer cone emission zones, and becomes larger when emission height decreases, that is, larger for inner cone and core component. When all the subpulses are summed up, the mean position angle will be the central value. So our model builds a natural connection between mean position angle and the projection of magnetic field lines as previously assumed.⁴ At the same time, a wider range

of position angles for subpulses from core component results in higher degree of depolarization of core component than conal components, which is the general case of observations.

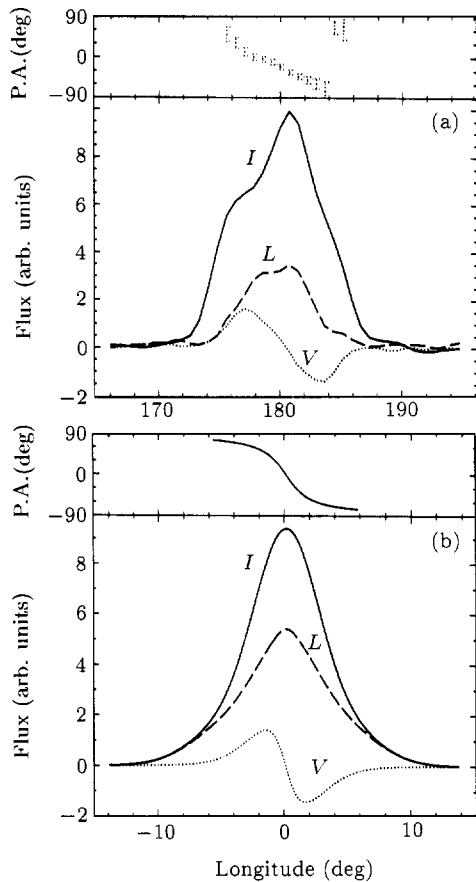


Fig. 2. Simulation of PSR1508+55 and comparison with observations; (a) is plotted with observational data at 925 MHz from European Pulsar Net. The pulsar period is 0.74 s, $\gamma_0 = 1000$, $\xi = 0.002$ and observation frequency is 1 GHz. (b) A S-shaped position angle swing, large amount of linear polarization and an antisymmetric type of net circular polarization are all present.

An observer can see bunches of particles all around his line of sight, while the polarization he receives from bunches in various positions is different. If bunches of particles appear all around the line of sight with equal probability, circular polarization will be canceled by incoherent summation of waves from all the bunches. In other words, there must be a steep and no radial

gradient in the probability of bunches' positions to give a net circular polarization. In inner gap model, the electric potential across the gap is produced via monopolar generation. When the magnetic axis tilts from the rotation axis, the potential across the part further from the rotation axis is different from that nearer to the rotation axis, resulting in different discharging probability for the two parts. We quote such an asymmetry in the simulation of PSR1508+55. The simulation and observations¹⁴ in comparison are presented in Fig. 2. An antisymmetric type of net circular polarization as well as linear polarization are obtained for this pulsar.

We conclude that coherent ICS explains the polarization behaviors of pulsar radio emission successfully. It also contributes to the unpolarized radiation since both summation of circular polarization of opposite sense and summation of linear polarization with diverse position angles may reduce the percentage of polarization. This means the coherent ICS may be responsible not only for linearly and circularly polarized radiation but also for unpolarized radiation, at least partially.

We thank Dr. J. L. Han, Dr. B. Zhang and Dr. B. H. Hong for helpful discussions and Mr. Z. Zheng for technical supports.

REFERENCES

- ¹ H. Lesch *et al.*, *Astron. Astrophys.* 332 (1998) 21.
- ² B. Zhang and G. J. Qiao, *Astron. Astrophys.* 310 (1996) 135.
- ³ J. M. Rankin, *Astrophys. J.* 274 (1983) 333.
- ⁴ V. Radhakrishnan and D. J. Cooke, *Astrophys. Lett.* 5 (1969) 21.
- ⁵ G. J. Qiao, in *High Energy Astrophysics*, edited by G. B. Bonner (Springer-Verlag, Berlin, 1988) p.88.
- ⁶ G. J. Qiao, *Vistas in Astronomy*, 31 (1988) 393.
- ⁷ G. J. Qiao and W. P. Lin, *Astron. Astrophys.* 333 (1998) 172.
- ⁸ R. X. Xu, Ph. D. Desertation, 1997, Peking University.
- ⁹ M. A. Ruderman and P. G. Sutherland, *Astrophys. J.* 196 (1975) 51.
- ¹⁰ J. M. Rankin, *Astrophys. J.* 405 (1993) 285.
- ¹¹ K. M. Xilouris *et al.*, *Astron. Astrophys.* 309 (1996) 481.
- ¹² R. N. Manchester *et al.*, *Mon. Not. R. Astron. Soc.* 295 (1998) 280.
- ¹³ J. L. Han *et al.*, *Mon. Not. R. Astron. Soc.* 298 (1998) (in press.)
- ¹⁴ D. M. Gould and A. G. Lyne, *Mon. Not. R. Astron. Soc.* 301 (1998) 235.